Armenian Journal of Physics, 2012, vol. 5, issue 2, pp. 86-94

INFLUENCE OF DEPOSITION RATE ON THE ELECTRICAL AND OPTICAL PROPERTIES OF ELECTRON-BEAM EVAPORATED InSb FILMS

Rahul*, A. K. Verma, R. S. N. Tripathi, S. R. Vishwakarma

Department of Physics and Electronics, Dr. R.M.L. Avadh University, Faizabad, India,

**E-mail- rhl.jaunpur@gmail.com*

Received 20 February, 2012

Abstract–Thin films of 300 nm thickness of non-stoichiometric indium antimonide ($In_{0.66}Sb_{0.34}$) have been deposited with different deposition rate onto well-cleaned glass substrate by electron beam evaporation technique. The electrical resistivity decreases with increasing temperature, showing the semiconducting behavior. Hall measurements indicate that the films were *n*-type, having carrier concentration ~10^{18} cm^{-3} and mobility ~10^3 cm^2/Vs for the film thickness of 300 nm with different deposition rate. Activation energy of the films with deposition rate is determined. The direct band gap has been calculated by Fourier transform infrared absorption spectra recorded at room temperature. The optical band gap varies in the range 0.21–0.23 eV with deposition rate of films.

***Keywords*:** InSb thin films; electron mobility; carrier concentration; electrical resistivity, optical band gap

1. Introduction

Preparation and characterization of compound semiconductors, especially of III-V group of elements play a major role in scientific research and its application. Among the III-V binary compound semiconductors, indium antimonide can show *n*-type and *p*-type semiconductivity, polycrystallinity and melts at 525°C. It is a narrow band gap semiconductor with an energy band gap of 0.17 eV at 300 K and 0.23 eV at 80 K [1-3]. In *n*-type indium antimonide (anion vacancy), the electrons have high electron mobility (80,000 cm^2/Vs), due to their smaller effective mass. Similarly in *p*-type InSb (cation vacancy), the holes have mobility 1250 cm^2/Vs. Therefore InSb is a suitable material for magnetic-field sensing devices such as Hall sensor and magnetoresistors [4], speed-sensitive sensors [5] and magnetic sensors [6]. The infrared detectors fabricated with *n*-type InSb thin films are sensitive in the 3–5 μm wavelengths [7]. These *n*-type InSb thin films can be also used as a bio-sensor to detect bacteria. Many reports are available on the growth of InSb thin films using different deposition techniques such as molecular-beam epitaxy (MBE) [8], metal organic chemical vapor deposition (MOCVD) [9], vacuum evaporation [10], liquid phase epitaxy [11] and sputtering [12]. The non-stoichiometry in thin films of indium antimonide is created during the deposition. The anion vacancies, i.e. indium enriched exhibit *n*-type semiconductivity and the cation vacancies exhibit *p*-type semi conductivity due to excess of antimony. The aim of the present study is to fabricate *n*-type indium antimonide thin films of 300 nm thickness with different deposition rate. This is a novel method to create controlled amount of non-stoichiometry in thin films. We have fabricated *n*-type $In_{0.66}Sb_{0.34}$ thin films by electron-beam evaporation technique using starting materials which have controlled non-stoichiometric composition. The electron-beam

evaporation technique is more suitable among physical evaporation technique because during the deposition materials come into vapor state without changing into liquid state. In this work we determined the electron mobility, carrier concentration, activation energy and optical band gap of thin films, study its variation with deposition rate and also optimized the deposition rate of thin films at room temperature.

2. Materials and Methods

2.1. Substrate Cleaning

The substrate cleaning play an important role in the deposition of thin films, so commercially available glass slide with size of (75 mm × 25 mm × 1 mm), washed in detergent, chromic acid and finally washed with double distilled water in ultrasonic cleaner and dry at 423 K in oven.

2.2. Preparation of Materials

Indium and antimony metal powders have been purchased from Alfa-Aesar Ltd. USA, having purity 99.999%. The starting materials having composition $In_{0.66}Sb_{0.34,}$ were used for fabrication of Indium antimonide thin films. To prepare the aforesaid compositional materials, desired molar ratios of $In_{0.66}$ (indium) and $Sb_{0.34}$ (antimony) metal powder were mixed by grinding with mortar rod and then mixed powder was heated at 50°C in vacuum unit (Hind Hivac Company. Ltd, India) using molybdenum boat under a vacuum 2×10^{-5} torr for ten hours and cooled up to room temperature under the same vacuum condition. This cooled sample again was grinded with mortar rod and heated under the same vacuum condition. This process is repeated five times with different temperature some higher than previous to this sample for formation of crystalline *n*-type InSb.

2.3 Preparation of InSb Thin Films

The $In_{0.66}Sb_{0.34}$ thin films of thickness 300 nm were deposited with different deposition rate onto a well cleaned glass substrate by electron beam evaporation technique under vacuum 10^{-5} torr, kept substrate temperature at 300 K. The prepared aforesaid non-stoichiometric starting material was taken in the graphite crucible and evaporated in vacuum ($\sim10^{-5}$ torr), where the vacuum system equipped with liquid nitrogen trap. Keep the source materials at 125 mm from the substrate holder. The deposition rate 3.0–18 nm/s was adjusted by changing the electrical current of electron beam gun. The deposition rate was measured by digital film thickness monitor using a quartz crystal sensor set at 6 MHz (DTM-10).

2.4 Electrical Property

The Hall Effect was studied by inducing a magnetic field perpendicular to the current flow direction in InSb thin films. Under such conditions, a Hall voltage is developed perpendicular to

both the current and magnetic field. The generated Hall voltage is described by following equation

$$\mathbf{F} = q\mathbf{E} + q\mathbf{V} \times \mathbf{B} \tag{1}$$

The Hall coefficient, carrier concentration and mobility are calculated by using measured Hall voltage and resistivity from following formulae [13]:

$$R_H = \frac{V_H \times t}{I_X B_Z}, \tag{2}$$

$$n = \frac{1}{R_H \times q}, \tag{3}$$

$$\mu = \frac{R_H}{\rho}, \tag{4}$$

where R_H is the Hall coefficient, n is the carrier concentration, μ is the mobility, V_H is the Hall voltage, *t* is the film thickness, I_X is the applied current in *x*-direction, B_Z is the applied magnetic field in *z*-direction and ρ is the resistivity of the film.

The applied magnetic field was measured by digital gauss meter (model DGM-204) and Hall voltage measured by digital micro voltmeter (model DMV-001).

The measurement of electrical resistivity of the samples has been done using standard four-probe method. A four-probe measurement is performed by making four linearly aligned electrical contacts to a sample surface through probe arranged in setup, two of the probes are used as a source current and remaining other two probes are used to measure voltage.

The electrical resistivity ρ is calculated by four-probe set up, applying a constant current *I* through the outer pair of probes and measuring the voltage drop *V* between the inner pair of probes which are positioned at a distance of $S = 0.2$ cm, using the following equation [13]:

$$\rho = \frac{V \times 2\pi S}{I \times C}, \tag{5}$$

where $C = 2S/t \log 2$, *t* is the thickness of the film, ρ is the resistivity.

2.5 Optical properties

Optical absorption of InSb thin films with different deposition rate were recorded using Fourier transform infrared spectrophotometer (FTIR, Perkin and Elmer, JASCO /4100) in wave length range 500–4500 nm from Department of Physics, the M.S.University, Vadodara, Gujarat.

The optical energy band gap of thin films was calculated by using Tauc relation [14]

$$\alpha h\nu = A(h\nu - E_g)^n \tag{6}$$

where, $h\nu$ is the photon energy, α is the absorption coefficient, E_g is the optical band gap, *A* is the constant, $n = 1/2$ for direct band gap material.

3. Results and discussion

3.1. Electrical analysis of InSb thin film

The values of Hall coefficient, electron mobility, carrier concentration, resistivity and activation energy of deposited $In_{0.66}Sb_{0.34}$ thin films at room temperature with different deposition rate were calculated and given in Table 1. The variation of Hall mobility with deposition rate is shown in Fig. 1. It is clear from Fig. 1 that the electron mobility increases with increasing deposition rate of the films and attains a maximum value of 10.375×10^3 cm^2/Vs at deposition rate 12 nm/s, which is attribute to the crystallite growth at higher deposition rates. The dependence of electron mobility on deposition rate may be due to variation in grain size [10].

Table 1. Electrical parameters of InSb thin films

Deposition rate (nm/s)	Hall coefficient $\times 10^1$/Coulomb	Mobility$\times10^3$ cm^2/Vs	Carrier concentration $\times 10^{18}/cm^3$	Resistivity$\times10^{-2}$ (Ohm cm)	Activation energy (eV)
3.0	1.389	2.106	0.450	0.66	0.067
6.0	2.231	4.300	0.280	0.52	0.058
9.0	3.416	7.591	0.183	0.45	0.052
12.0	4.254	10.375	0.147	0.41	0.047
15.0	4.227	10.064	0.148	0.42	0.048
18.0	4.151	9.434	0.150	0.44	0.050

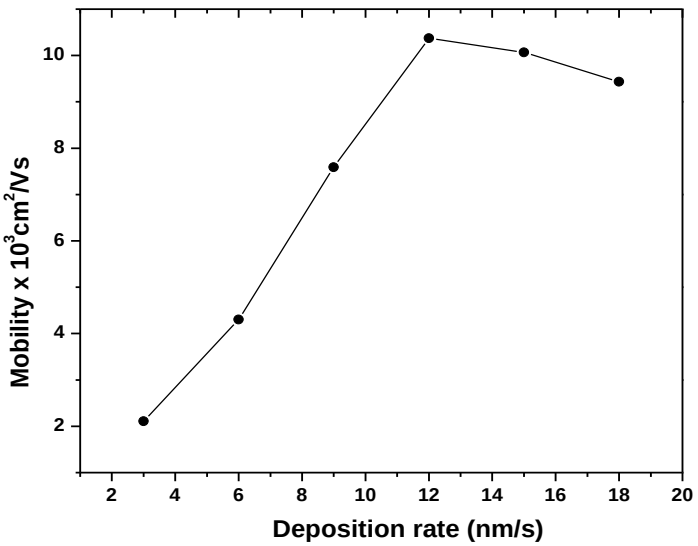

Fig. 1. Variation of Hall mobility with deposition rate for a film of 300 nm thickness at room temperature

Fig. 2 shows the variation of carrier concentration with deposition rate. It is found from Fig. 2 that the carrier concentration decreases with increasing deposition rate till 12 nm/s and thereafter it nearly becomes saturate with increase of deposition rate. The variation of Hall coefficient with film deposition rate is shown in Fig. 3. It is clear from Fig. 3 that the Hall coefficient increases with increasing film deposition rates till 12 nm/s and thereafter it slowly decreases with increase of deposition rate.

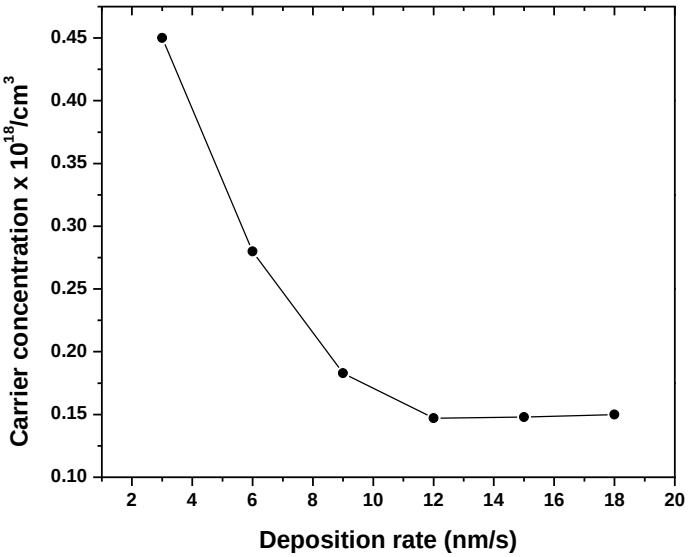

Fig. 2. Variation of carrier concentration with deposition rate for a film of 300 nm thickness at room temperature

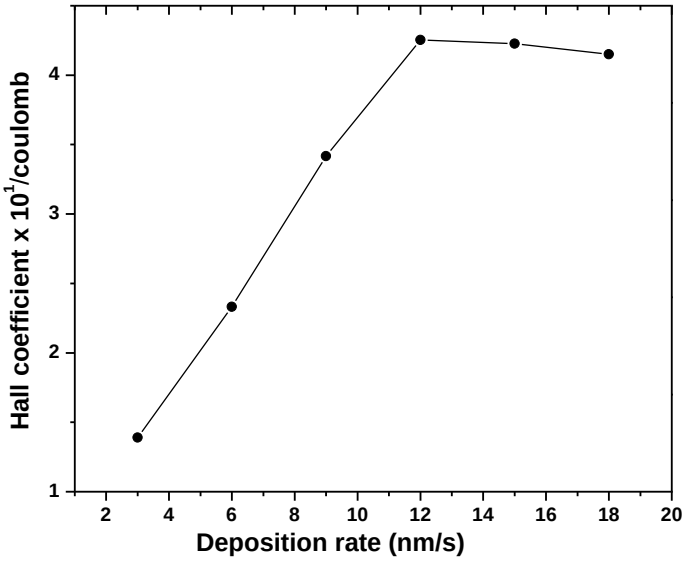

Fig. 3. Variation of Hall coefficient with deposition rate for a film of 300 nm thickness at room temperature

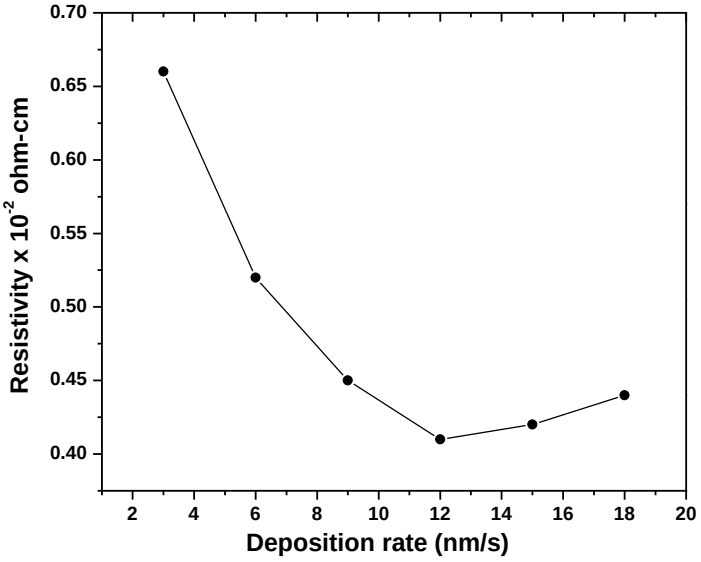

Fig. 4. Variation of resistivity with deposition rate for a film of 300 nm thickness at room temperature

Fig. 4 shows that the variation of films resistivity with deposition rate. It is found from Fig. 4 that the resistivity decreases with increasing film deposition rates till 12 nm/s, thereafter it slowly increases with increasing deposition rates. This is explained in terms of structural changes in this film with deposition rate, i.e. size of grains increases with deposition rate and also conductivity increases because conductivity is directly proportional to the grain size [15].

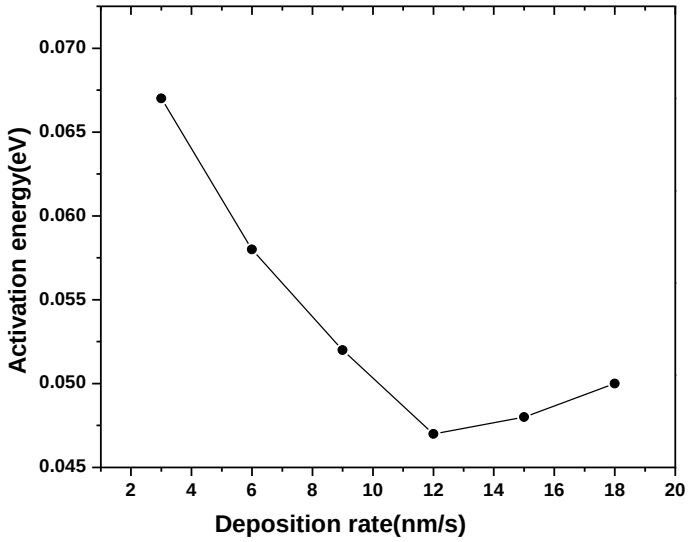

Fig. 5. Variation of activation energy with deposition rate for a film of 300nm thickness at room temperature

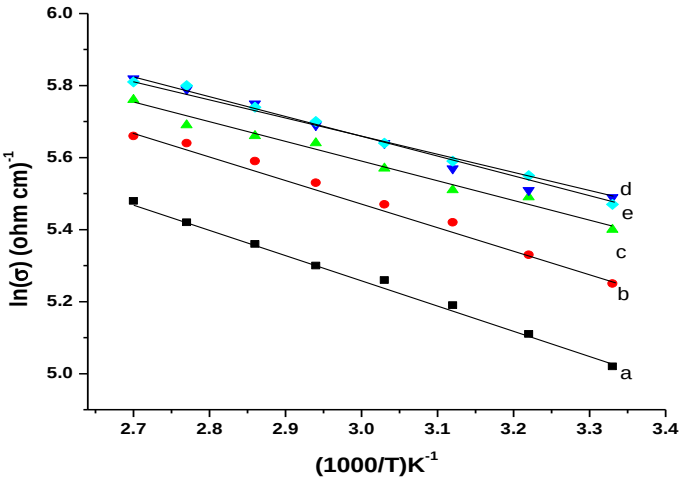

Fig. 6. Variation of $\ln\sigma$ (Ohm cm)$^{-1}$ with 1000/T K^{-1} at different deposition rate: (a) 3nm/s, (b) 6nm/s, (c) 9nm/s, (d) 12nm/s, (e) 15nm/s.

Fig. 5 shows the variation of activation energy with different deposition rate. Initially it decreases with deposition rate till 12 nm/s and thereafter it slowly increases with deposition rate. Fig. 6 shows that the variation of $\ln\sigma$ (Ohm cm)$^{-1}$ with 1000/T K^{-1} at different deposition rate of the films thickness 300 nm. It is clear from Fig. 6 that the conductivity increases with temperature and shows a semiconducting behavior. In present study the obtained values of electrical parameters such as electron mobility, carrier concentration of deposited thin films were low because deposited

films are at room temperature and films have some structural defects [10,16]. The carrier concentration and Hall mobility of the films observed in the present study is in agreement with the observation of Wieder [17], Kim [18] and Matsumoto [19]. The activation energy obtained in present investigation is similar to that observed by other investigator [20].

3.2. Optical Analysis of InSb Thin Films

Fourier transform infrared [FTIR] spectra for *n*-type InSb thin films with different deposition rate at room temperature are shown in Fig. 7. It is clear from Fig. 7 that the optical absorption increases with different deposition rate of the films. The variation of $(\alpha h\nu)^2$ with photon energy for InSb thin films of 300 nm thickness with different deposition rate at room temperature are shown in Fig. 8. Since the material is direct band gap, so in the present work we have used $n = 0.5$. It is clear from Fig. 8 that the extrapolation of straight-line portion to $(\alpha h\nu)^2 = 0$ axis gives the value of direct band gap of thin films. It is observed from Fig. 8 that the direct band gap varies in the range 0.21–0.23 eV with deposition rates of the films and attain minimum direct band gap 0.21 eV at 12 nm/s deposition rate. The observed optical direct band gap can be explained on the basis of the reduction in the number of unsaturated defects, decreases in density of localized state in the band structure of the films. These direct band gap obtained in present investigation are slightly higher to those observed by other investigators [1,3].

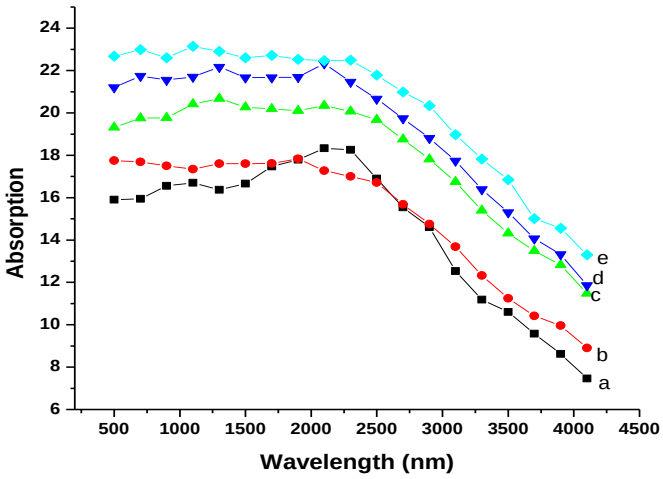

Fig. 7. Variation of absorption with wavelength (nm) for a film of 300 nm film thickness with rate: (a) 3.0nm/s, (b) 6.0 nm/s, (c) 9.0 nm/s, (d) 12.0 nm/s, (e) 15.0 nm/s.

Scanning electron micrographs (SEM) have been used for the analysis of surface morphology of *n*-type InSb thin films. The SEM pictures of *n*-InSb films on glass substrate are shown in Fig. 9. It is clear from micrographs that the deposited *n*-InSb films are homogenous, without cracks or holes, well covered to the glass substrate.

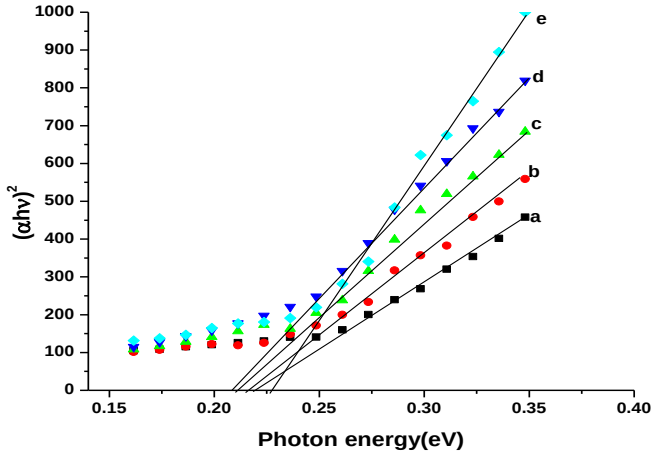

Fig. 8. Variation of $(\alpha h\nu)^2$ with photon energy for a film of 300 nm thickness with different deposition rate: (a) 3 nm/s, (b) 6 nm/s, (c) 9 nm/s, (d) 12 nm/s, (e) 15 nm/s.

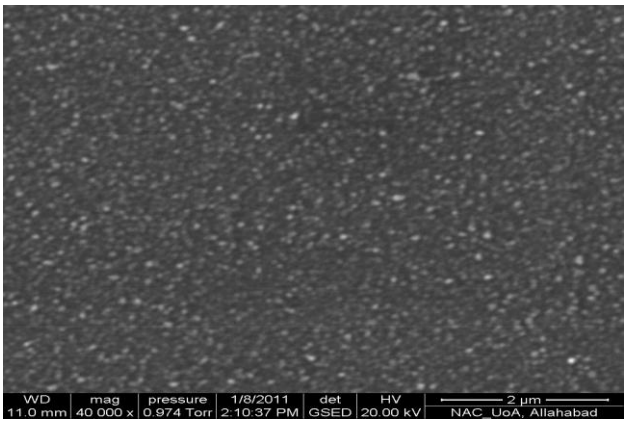

Fig. 9. Typical SEM image of InSb thin film

4. Conclusions

The non-stoichiometric indium antimonide thin films of 300 nm thickness were deposited at room temperature with different deposition rate onto glass substrate using prepared non-stoichiometric starting materials by electron-beam evaporation technique. Hall measurements show that films have *n*-type semiconductivity. The electron mobility increases but films resistivity, activation energy and optical band gap decreases with increasing deposition rate. Thin films deposited at 12 nm/s deposition rate are optimized due to its electrical and optical properties.

Acknowledgements

The financial support has been provided by U.P. Council of Science and Technology, Lucknow, India. Authors are thankful to Prof. K. Singh, Department of Physics and Electronics, Dr. R.M.L. Avadh University, Faizabad for providing necessary facilities. Authors are also grateful to Dr. S.R. Vishwakarma for help in film preparation and its characterizations.

REFERENCES

1. **R.K.Mangal, Y.K.Vijay,** Bull Mater Sci, **30**, 117 (2007).
2. **R.K.Mangal, B.Triapthi, M.Singh, Y.K.Vijay, A.Rais,** Indian J Pure Appl. Phys., **4**5, 987 (2007).
3. **R.K.Mangal, Y.K.Vijay, D.K.Avatshi, B.R.Shekhar,** Indian J. Eng. Mater. Sci., **14**, 253 (2007).
4. **J.Heremans, D.L.Partin, C.M.Thrush,** Semi Sci. Technol., **8**, 424 (1993).
5. **M.K.Carpenter, M.W.Verbrugge,** J Mater Res, **9**, 2584 (1994).
6. **A.Okamoto, T.Yoshida, S.Muramatsu, I.Shibasaki,** J. Cryst. Growth, **201**, 765 (1999).
7. **N.K.Udayshankar, H.L.Bhat,** Bull Mater. Sci., **24**, 445 (2001).
8. **T.Zhang, S.K.Clowes, M.Debnath, A.Bennett, C.Roberts, J.J.Harris, R.A.Stradling,** Appl. Phys. Lett., **84**, 22 (2004).
9. **D.K.Gaskill, G.T.Stauf, N.Bottka,** Appl. Phys. Lett., **58**, 1905 (1991).
10. **Md.A.Taher**, Daffodil Int. University J. Sci. Techn., **2**, 39 (2007).
11. **D.E.Holunes, G.S.Kamnath,** J. Electron. Mater., **9**, 95 (1980).
12. **T.Miyazaaki, M.Kunugi, Y.Kitamure, S.Adachi,** Thin Solid Films, **287**, 51 (1996).
13. **M.S.Tyagi,** Introduction to Semiconductor Materials and Devices, John Wiley and Sons, 1991.
14. **M.Singh, Y.K.Vijay,** Indian J. Pure Appl. Phys., **42**, 610 (2004**).**
15. **S.M.Sze,** Physics of Semiconductor Devices, **Ed.2**, New Delhi, H.S.Poplai, Wiley Eastern Ltd, 31, 1993.
16. **V.Senthilkumar, S.Venkatachalam, C.Viswanath, K.C.Wilson, K.P.Vijayakumar,** Cryst. Res. Technol, **40**, 573 (2005).
17. **H.H.Wieder,** J. Vacuum Sci. Tech., **8**, 210 (1981).
18. **W.Y.Kim, C.Joonyeon, S.H.Han,** J. Appl. Phys., **97**, 10D507 (2005).
19. **M.Mori, N.Fujimoto, N.Akae, K.Uotani, T.Tambo, C.Tatsuyama,** J. Cryst. Growth, **286**, 218 (2006).
20. **S.K.J.Ani, Y.N.Obaid, S.J.Kasim, M.A.Mahdi,** Int. J. Nanoelectronics and Materials, **2**, 109 (2009).